Differential expression of microRNAs and potential targets under drought stress in barley

Running title: miRNA expression under drought in barley

Jannatul Ferdous[1, 2], Juan Carlos Sanchez-Ferrero[1, 3], Peter Langridge[2], Linda Milne[4], Jamil Chowdhury[2,5], Chris Brien[3], and Penny J. Tricker[1, 2]*

Authors' Affiliations

[1] Australian Centre for Plant Functional Genomics, PMB1, Glen Osmond, SA 5064. Australia

[2] School of Agriculture, Food and Wine, The University of Adelaide, PMB1, Glen Osmond, SA 5064. Australia

[3] Phenomics and Bioinformatics Research Centre, School of Information Technology and Mathematical Sciences, University of South Australia, Mawson Lakes SA 5095, Australia

[4] The James Hutton Institute, Invergowrie, Dundee DD2 5DA, Scotland U.K.

[5] ARC Centre of Excellence in Plant Cell Walls, The University of Adelaide, Waite Campus, Glen Osmond, SA, Australia

*Author for correspondence

Corresponding author contact details

Dr Penny Tricker. Address: Australian Centre for Plant Functional Genomics, Plant Genomics Centre, Hartley Grove, Urrbrae, South Australia 5064, Australia.

Email: penny.tricker@adelaide.edu.au

Telephone: +61 8 8313 7180

ABSTRACT

Drought is a crucial environmental constraint limiting crop production in many parts of the world. microRNA (miRNA) based gene regulation has been shown to act in several pathways, including crop response to drought stress. Sequence based profiling and computational analysis have revealed hundreds of miRNAs and their potential targets in different plant species under various stress conditions, but few have been biologically verified. In this study, eleven candidate miRNAs were tested for their expression profiles in barley. Differences in accumulation of only four miRNAs (*Ath*-miR169b, *Osa*-miR1432, *Hv*-miRx5 and *Hv*-miR166b/c) were observed between drought-treated and well-watered barley in four genotypes. miRNA targets were predicted using degradome analysis of two, different genotypes and genotype-specific target cleavage was observed. Inverse correlation of mature miRNA accumulation with miRNA target transcripts was also genotype-dependent under drought treatment. Drought-responsive miRNAs accumulated predominantly in mesophyll tissues. Our results demonstrate genotype-specific miRNA regulation under drought stress and evidence for their role in mediating expression of target genes for abiotic stress response in barley.

Keywords: *Hordeum vulgare*, genotype, canonical cleavage, degradome, *in situ*-RT-PCR.

INTRODUCTION

In many regions of the world, crop production is constrained by prolonged dry conditions. Declining water resources and increased variation in rainfall will require the development of climate-resilient crop varieties. One of the visions of plant stress research is to provide genetic loci as targets for enhancing stress tolerance in crop plants. A key step in the development of stress tolerant crop varieties will be understanding of the function of stress-

responsive genes. Improved understanding of gene regulation during stress could aid the development of genomic tools (Langridge and Reynolds, 2015). One of the central molecules for naturally occurring regulation of gene transcription is microRNA (miRNA). miRNAs are non-coding transcripts of 18-21 nucleotides (nt) in length. Generally, plant miRNAs function in a sequence specific mode to target mRNAs based on complementary base pairing, leading to cleavage of the target mRNA (Lee *et al*., 1993; Reinhart *et al*., 2002) and it has been suggested that miRNAs play a regulatory role in activating stress defence or response gene networks (Zhu, 2002).

The identification of miRNAs is an essential precursor to understanding and quantifying their roles in regulating mRNA. Large-scale bioinformatic analysis has enabled miRNA discovery in plants such as *Arabidopsis*, *Medicago*, *Brachypodium* and, more recently, crop plants like rice, maize, wheat and barley According to miRBase (miRBase v. 20; Kozomara and Griffiths-Jones 2014), to date 7385 mature miRNA sequences from 72 plant species have been identified. Families of miRNAs may be conserved between species and taxa but unique miRNAs have also been discovered in each species analysed (Schreiber *et al*., 2011). Although many miRNAs have been identified, the regulation of miRNA expression is still poorly understood and the existence of multiple isoforms of mature miRNAs generated from a single miRNA locus complicates analysis and, hence, understanding of miRNAs' functional relevance (reviewed in Budak *et al*., 2015).

The quantification of mature miRNA expression is difficult due to their short length and absence of common sequence features (e.g. polyA) (Benes and Castoldi, 2010). Some mature miRNAs are difficult to distinguish as they differ by as few as one or two nucleotides and technical limitations may hinder discovery when protocols are unable to distinguish between mature miRNAs and their precursors (Li *et al*., 2014), or closely related miRNAs that are very similar in sequence (Balcells *et al*., 2011). Thus expression of an abundant

miRNA may mask the expression of a low abundance or very similar miRNA. Stem-loop qRT-PCR has proven a reliable technique for the detection of mature miRNAs (Chen *et al*., 2005, Varkonyi-Gasic *et al*., 2007; Shen *et al*., 2014), though the limitation of this technique is that it requires a separate reverse transcription (RT) reaction for each miRNA.

A key objective of miRNA expression profiling is to identify and validate the miRNA's target mRNAs, but this can be challenging if it depends solely on predictions using computational approaches. In plants, miRNA regulated gene expression occurs by target mRNA cleavage (Baumberger and Baulcombe, 2005; Jones-Rhoades *et al*., 2006) or by inhibition of target mRNA translation (Gu and Kay, 2010; Vazquez *et al*., 2010). miRNA directed mRNA cleavage occurs when there is perfect or near perfect Watson-Crick complementary pairing between the miRNA and target mRNA (Zhang *et al*., 2006; Krol *et al*., 2010). However, perfect pairing between the miRNA and the target is neither obvious nor sufficient for the miRNA: target interaction (Brennecke *et al*., 2005; Witkos *et al*., 2011; Künne *et al*., 2014).

The prediction of miRNA targets using computational programs based on sequence alignment has been used frequently. There are a variety of important parameters for *in silico* prediction including alignment score, maximum score, number of consecutive mismatches, number of G:U wobble pairing and number of gaps (Zhang *et al*., 2006; Xie and Zhang, 2010; Dehury *et al*., 2013). Upon base-pairing, miRNA guided mRNA cleavage occurs at its site opposite the 5' end at the 10th and 11th positions of the miRNA (Huntzinger & Izaurralde, 2011). Using these parameters, the *in silico* prediction of targets, followed by validation using a sequenced small RNA library of degraded transcripts (degradome analysis) helps to shortlist the candidate target genes. It is worth mentioning that the targets of miRNAs may not be conserved across different plants species, although miRNAs are (Lu *et al*., 2005). Therefore, the targets of miRNAs need to be validated in individual plant species.

Despite technical hurdles to miRNA functional analysis, there is a growing body of evidence that alteration of miRNA accumulation plays an important role in reprogramming plant responses to biotic and abiotic stresses (Berger *et al*., 2009; Hackenberg *et al*., 2013). Drought stress has been revealed to alter the expression of many miRNAs. For example, differential expression of miR398a/b under drought was observed in *Medicago truncatula* in two different studies (Trindade *et al*., 2010, Wang *et al*., 2011). Members of the miRNA family miR319 were also found to be differently expressed under drought stress in rice (Zhou *et al*., 2010). miR166 was up-regulated in drought-stressed barley (Kantar *et al*., 2010) and down-regulated in wild emmer wheat (Kantar *et al*. 2011); miR171 was induced in barley (Kantar *et al*., 2010) and reduced in wheat (Kantar *et al*. 2011) under drought shock. The differential miRNA abundances under drought revealed in these studies suggest a role for miRNAs in reprogramming plant responses to drought stress, and differential miRNA expression may govern the fine tuning and control of stress signalling (Gutierrez *et al*. 2009).

Barley is not only an economically important crop, but is also well known for its genotypic variability under adverse conditions. Hence, it is an excellent model plant to study drought response and to identify and analyse functions of drought responsive miRNAs. Although deep-sequencing technology has extended the discovery of barley miRNAs (Schreiber *et al*., 2011; Hackenberg *et al*., 2015), only a limited number of studies have investigated miRNAs in barley under drought stress (Kantar *et al*., 2010, Hackenberg *et al*., 2015). It is often not clear which mature miRNAs are truly drought responsive and what is the mode of function of these miRNAs to regulate their target gene(s). Information about the spatial patterns of drought responsive mature miRNAs and their targets could help our understanding of the molecular events involved in the drought stress response. If miRNAs are to be used in enhancing the drought tolerance of crop plants, we need to establish both function and evidence for genetic variation in their expression. Therefore, our aims in this

study were to evaluate drought responsive miRNA expression in different barley genotypes under drought, to identify and validate the target genes, and to determine the cellular localization of important drought responsive miRNAs and their targets. We validated miRNAs associated with drought response in four genotypes (*Hordeum vulgare* L. 'Commander', 'Fleet', 'Hindmarsh' and breeding line WI4304) that showed similar performance in drought prone areas of Australia (Fettell, 2011; Coventry *et al*., 2012). We predicted potential miRNA targets using degradome libraries and validated both the predicted drought-responsive miRNAs and their targets using qRT-PCR. *In situ* –RT-PCR (ISRT-PCR) was performed to localize expression of selected miRNAs and their targets. Identifying miRNAs associated with drought response and recognizing their targets in different barley genotypes could help determine the potential contribution of miRNAs for the varietal selection of stress tolerant crop plants.

MATERIALS AND METHODS

Plant materials and drought treatment

Plants were grown in a growth chamber maintained at 23 °C day and 18 °C night temperatures, 12 h/12 h light/dark photoperiod, 450 µmol m^{-2} s^{-1} Photosynthetically Active Radiation and 60 % Relative Humidity. Seeds were germinated on petri dishes and seedlings that germinated at the same time and were of the same physiological stage were transplanted to pots. Twenty four pots were used where each pot contained four plants, one each of *Hordeum vulgare* L. cvs. 'Commander', 'Fleet', 'Hindmarsh' and breeding line WI4304, to minimize the inter pot variation. Three weeks after transplanting half the pots were subjected to drought treatment of -6 bar soil water potential, while control pots were maintained at -2.5 bar, with watering to weight for a further six weeks. The interaction between treatment and development was significant so that well-watered plants reached maturity faster (47.5 d ±1)

than drought-treated plants (57.8 d ±1) (supporting information Fig. S1) so samples were collected at a defined, physiological stage (booting) from each plant. The flag leaf was harvested from the drought-stressed and well-watered plants of five replicates and immediately frozen in liquid nitrogen and stored at −80 °C. From 12 plants in each treatment per genotype, two fully expanded mature leaves (per plant) were sampled to record the leaf water potential (LWP) and the relative water content (RWC) respectively, for no more than two hours at and after solar noon. There were no significant differences in the dry weights of mature, sampled leaves between genotypes or treatments. The fresh weights of sampled leaves differed with treatment with drought-treated leaves weighing less, but there were no significant differences between the genotypes within a treatment (supporting information Fig. S2).

Leaf water potential measurement

LWP was measured using a pressure chamber (Scholander Pressure Chamber Model 3000) and the method of Boyer (1967). A fully expanded, mature leaf was cut and placed immediately through the chamber lid with the cut end of the leaf outside and the remaining part of the leaf inside the chamber. Pressure was increased slowly. A magnifying glass was used to observe the cut end of the leaf. As soon as a drop of sap appeared from the cut end of the leaf sample, the pressure shown on the chamber gauge was recorded as a measure of the LWP (Boyer, 1967).

Relative Water Content measurement

RWC was determined by the method of Barrs and Weatherley (1962). The mid-leaf section of a fully expanded leaf was weighed to determine fresh weight (FW). Then samples were re-hydrated overnight and the turgid weight was (TW) recorded. Samples were oven dried at

80°C for 24h and weighed to determine dry weight (DW). RWC (%) was calculated using the formula [(FW-DW) / (TW-DW)] x 100.

Primer designs

The selection of miRNAs used in this study was based on barley miRNAs identified by Kantar *et al*. (2010), Schreiber *et al.* (2011), Hackenberg *et al.* (2012) and Hackenberg *et al.* (2015). Selected miRNAs had previously been shown to be differential expressed under drought in leaves or shoots of different species including barley (*Hv*-miR166b/c, *Ath*-miR169b, *Osa*-miR393a, *Hv*-miR444b, *Hv*-miR5048a, *Hv*-miR171), *Medicago truncatula*, *Oryza sativa*, *Prunus persica*, *Populus euphratica* and *Triticum turgidum* ssp. *dicoccoides* (reviewed in Ferdous *et al*., 2015a) except *Hv*-miRx5 and *Ata*-miR9863a. Stem-loop reverse transcription (RT) primers were used for cDNA synthesis from mature miRNAs. Primer sequences and miRNA identities are given in Table 1. miRNA specific stem-loop RT primers, and forward and reverse primers for individual miRNAs were designed following the method established by Chen *et al.* (2005) and refined by Varkonyi-Gasic and colleagues (2007) where the last 3′ six nt of a miRNA sequence was used as the antisense overhang, and the miRNA specific forward primer was designed to contain the remaining 5′ sequences (normally 13-15 nt from the 5′ end of the specific miRNA). We considered up to three nucleotides of these remaining 5′ sequences which were not contained by the forward primer and were used as the signature nucleotides to verify the respective miRNA by sequencing.

For quantification of mRNA targets in the same RNA samples, primers were designed to span the target site; that is, including the miRNA: target pairing region and primers were *NFY-A*:

forward: 5′ CATCACGGTCACCATCTC 3′ and reverse: 5′ ATCTCTGAAGTCCTAACACG 3′; and *EF hand* containing transcript: forward: 5′

ATATCACCACAAGCGTTCAC 3′ and reverse 5′ GAGCGAGATCAGGAGAGAC 3′. Primer efficiencies and unique products were confirmed by a single, distinct peak in melt curve analysis (Supporting Information Fig. S3).

miRNA and target mRNA analyses using qRT-PCR

Total RNA was extracted from leaves using TRIzol reagent (Invitrogen, Carlsbad, CA, USA) according to the manufacturer's instructions. To remove genomic DNA contamination, RNA samples were treated with DNA-free™ (Ambion, Life Technologies, Grand Island, NY, USA) twice according to the manufacturer's instructions. The concentration and integrity of the DNase treated RNA was measured with an Agilent-2100 Bioanalyzer (Agilent Technologies, Santa Clara, CA, USA). The RNA integrity number (RIN) was higher than 6 for all samples.

One μg total RNA from each sample was reverse transcribed to cDNA using SuperScript® III RT (Life Technologies, Carlsbad, CA, USA) and gene specific primers (Table 1). cDNA synthesis for miRNAs was carried out following the method described by Varkonyi-Gasic *et al*., (2007). We used up to six stem-loop primers [1 μl of miRNA specific stem-loop RT primer each (1 μM)] in one RT reaction. The RT reaction also contained 10 μM of anti-sense primers for internal controls (Ferdous *et al*., 2015b). Gene specific primers were also used for target cDNA synthesis using SuperScript® III RT (Life Technologies, Carlsbad, CA, USA) and following the manufacturer's instructions for the RT reaction.

miRNA and target qRT-PCR assays were carried out exactly as in Ferdous *et al.* (2015b) using the RG6000 Rotor-Gene real-time thermal cycler (Qiagen, Valencia, CA, USA) with 2 min at 95 °C, followed by 50 cycles of 1 second at 95 °C, 1 second at 60 °C, 25 seconds at 72°C, and fluorescence acquisition at 72°C. Five independent plants were used for each treatment per genotype with three technical replicates per biological replicate.

miRNA qRT-PCR products were sequenced using M13 reverse primers following the method described by Ferdous *et al.*, (2015b) to verify signature nucleotide(s) (Supporting Information Fig. S4). qRT-PCR amplicons of uncleaved targets were also verified in each genotype by Sanger sequencing.

Statistical design and analysis

A split-plot design was used where pots were the main plots and each pot was divided into four quadrants to give four subplots (Supporting Information Fig. S5). The experiment involved 24 pots arranged in four rows by six columns to give a total of 96 plants. The watering conditions were assigned to the pots using two 6 × 6 Latin squares. An analysis of variance was performed on all data variables. The blocking structure of the analyses (excluding qRT-PCR data), derived from the design, was (Rows*(PairsColumns/WithinColumns))/Quadrants. For the qRT-PCR data, five replicates were used and the only blocking structure included in the analysis was pot number. This accounted for variability between pots and similarities between qRT-PCR materials from quadrants of the same pot. The overall significance tests used an F test-statistic and tests for significance between means were conducted using a least significant difference (LSD) value at the 5% significance level.

Target prediction and validation by degradome analysis

Target prediction of the drought responsive miRNAs was first conducted *in silico*. We searched the miRNA sequences against an RNA sequencing dataset from 16 tissues and growth stages in barley from the James Hutton Institute (unpublished data) and from Ensembl Plants using psRNATarget (http://plantgrn.noble.org/psRNATarget/) and the parameters Dehury *et al*., (2013) were i) maximum expectation: 4.0 (range: 0-5.0), ii) length for

complementary scoring (hspsize): 20 (range: 15-30bp), iii) target accessibility - allowed maximum energy to un-pair the target site (UPE): 25 (range: 0-100, less is better), iv) flanking length around target site for target accessibility analysis: 17 bp in upstream/13 bp in downstream, v) range of central mismatch leading to translational inhibition: 9 - 11 nt. The predicted targets of 11 miRNAs were classified based on their gene ontology (GO) and Pfam annotation.

Two barley degradome libraries were analysed: one from the cv. 'Golden Promise' was described by Hackenberg *et al*. (2015) and an additional cv. 'Pallas' was also used. Sequencing libraries were prepared from the pooled samples of leaves and roots of well-watered and drought treated plants according to the method described by Addo-Quaye *et al*. (2008). RNAs were first isolated using the Oligotex Kit (Qiagen, Santa Clarita, CA, USA) then ligated with a 5' RNA adaptor containing a MmeI restriction site using T4 RNA ligase. After reverse transcription of the ligated products, second-strand synthesis and MmeI digestion, ligation of a 3' dsDNA adaptor and gel-purification, the cDNAs were amplified by PCR and sequenced on the Illumina HiSeq platform.

To validate the targets, degradome sequence reads were mapped to the target RNA sequences using Biokanga v3.4.3 (http://sourceforge.net/projects/biokanga/) with default parameters set to obtain all perfect alignments to the cleavage product starting at the canonical (10–11 nucleotide) positions of the miRNAs. We allowed for a single nucleotide variation between varieties and 1 nt length difference between the degradome sequence and the reference mRNA sequence. The miRNAs of interest were also aligned to the reference mRNA sequences using BLAST+ v2.2.28 (Camacho *et al.*, 2009). Integrative Genomics Viewer (IGV) (Robinson *et al.*, 2011) was used to load the alignments for manual inspection.

***In situ* PCR**

Transcript localization of miRNAs and targets was performed through *in situ* PCR in formalin-fixed paraffin-embedded (FFPE) leaf sections. Sample and reagent preparation were carried out combining the protocols described by Przybecki *et al*., (2006), Bagasra (2007), Møller *et al*., (2009) and Athman *et al*., (2014) with some modifications. Flag leaf samples from drought and well-watered conditions were fixed with fresh FAA fixative. Samples were embedded in paraffin and the Leica RM2265 Rotary Microtome (Leica Microsystems, North Ryde, Australia) was used for sectioning and subsequent treatments on slide. *In situ* reverse-transcription of miRNAs and targets was carried out in the DNase treated leaf sections using SuperScript® III RT (Life Technologies, Carlsbad, CA, USA) according to the manufacturer's instruction except that the miRNA RT preparation and conditions were as described by Varkonyi-Gasic *et al* (2007). PCR was carried out using NEB Taq DNA Polymerase (New England Biolabs, Ipswich, MA, USA) with Standard Taq Buffer according to the manufacturer's instruction for a final volume of 60 µl, containing 4 µM final concentration of Digoxigenin-11-dUTP (Roche Diagnostics, Alameda, CA, USA) as an additional reagent. For the respective negative controls, the same primers and conditions were used using RNA as templates in the PCR reactions. PCR and post-PCR treatment were conducted as described by Athman *et al*. (2014). Following colorimetric detection, the sections were mounted with ImmunoHistoMount™ (Sigma-Aldrich, Castle Hill, NSW, Australia), dried and were visualized in the Zeiss Axio Imager M2 microscope (Carl Zeiss, Oberkochen, Germany) under bright field Illumination. The images were captured using the AxioCam ERc5s camera and retrieved using ZEN 2011 software (Carl Zeiss, Oberkochen, Germany) while the exposure time was adjusted to 100 ±20 ms for each specimen. The details of the *in situ* PCR method are described in the Supporting Information (File S1).

RESULTS

Response of four barley genotypes to drought treatment

Two physiological parameters, leaf water potential (LWP) and leaf relative water content (RWC) were measured under drought treatment and in well-watered conditions. The LWP dropped significantly in all genotypes under drought (Fig. 1a). Hindmarsh had higher RWC compared with the other three genotypes (Fig. 1b).

qRT-PCR analysis of candidate drought responsive miRNAs in barley leaves

Quantification of 11 candidate mature miRNAs was performed in five biological replicates from each genotype. Among the 11 miRNAs, four miRNAs (*Ath*-miR169b, *Osa*-miR1432, *Hv*-miRx5 and *Hv*-miR166b/c) showed differential expression under drought. The homologous miRNA *Ath*-miR169b was significantly induced under drought in Hindmarsh and WI4304 (Fig. 2a). The miRNA homologous to *Osa*-miR1432 was significantly down under drought in Commander, Fleet and Hindmarsh (Fig. 2b). Two barley miRNAs, miRx5 (Fig. 2c) and miR166b/c (Fig. 2d) were significantly reduced under drought only in Commander, but did not change between drought-treated and well-watered samples in the other three genotypes. Three miRNAs *Osa*-miR393a (Fig. 2e), *Ata*-miR9863 (Fig. 2f) and *Bdi*-miR396b (Fig. 2g) and two barley miRNAs *Hv*-miR5048 (Fig. 2h) and *Hv*-miR444b (Fig. 2i) did not show significant variation between well-watered and drought treated plants in any of the four genotypes. There were no significant differences in expression detected for miR169n (a rice homologous miRNA) and miR171 (a barley miRNA) with drought treatment, and these two miRNAs had very low abundance in the leaf tissue of the genotypes used in this study (Fig. 2j & k).

Drought responsive miRNA targets

We detected the putative targets of the 11 chosen miRNAs using RNA sequence data. We identified ~400 putative target transcripts for 11 miRNAs (Supporting Information Table S1). The putative barley drought-responsive miRNA targets had a diverse range of functions (Supporting Information Table S1) and more than one target was predicted for each miRNA so that further experimental confirmation was required.

Among the predicted targets for the 11 miRNAs, we were able to obtain 15 target sequences for nine miRNAs that had cleavage products in the degradome libraries (Table 2). Degradome analysis demonstrated alignment positions consistent with miRNA directed cleavage of mRNA targets; that is, where the start of one or more degradome reads coincided preferentially with the canonical 5' 10-11 nt cleavage site for the mature miRNA sequence (Fig. 3a-b; Supporting Information Fig. S6 a-m). An NFY-A encoding gene was cleaved by both *Ath*-miR169b and *Osa*-miR169n, and the cleavage products were obtained in libraries from both barley cvs. Golden Promise and Pallas. Interestingly, we observed a mismatch between the miRNA and the target at the seed region (the 5′ 2-8 nt of a miRNA) which was found in the genotype Pallas (Fig. 3a and Supporting Information Fig. S6 e). An mRNA encoding a Calmodulin-related (EF hand containing) calcium sensor protein appeared to be cleaved by *Osa*-miR1432 in Golden Promise (Fig. 3b). The cleavage products of mRNAs from four genes encoding homeobox START and MEKHLA domain containing proteins were the apparent targets of *Hv*-miR166b/c in Golden Promise. mRNAs from two genes encoding LRR domain containing F box proteins showed *Osa*-miR393a mediated cleavage products in both Golden Promise and Pallas. Cleavage products of mRNA targets for WRC and QLQ domain proteins were found for *Bdi*-miR 396b in Golden Promise and Pallas. An mRNA from a MADS box family gene was found to be targeted by *Hv*-miR444b both in Golden Promise and Pallas. However, the degradome product did not match the canonical site and was at the 5' 19-20 nt position opposite to the miRNA suggesting that the miRNA-

mediated cleavage sites may not have been limited to 10-11 nt position. *Hv*-miR5048a was found to cleave the transcript encoding a serine/threonine-protein kinase receptor in Golden Promise. mRNAs from two genes encoding NB-ARC domain containing protein were cleaved by *Ata*-miR9863 in both libraries. We did not identify any cleavage products aligned with either degradome library for the candidate targets of miR171. For miRx5 target validation, we obtained cleavage products aligned with miRx5's predicted target *RGH1A*, starting at the 5' 5-6 nt position of the miRNA/target duplex, opposite to the miRNA in Golden Promise (Supporting Information Fig. S6 n). This region was clearly the seed region of a miRNA. It was unlikely that target cleavage occurred on the opposite strand to the seed region of this miRNA. Moreover, the G:U wobble pairing at the 11 nt position between the miRx5 and its target might have obstructed target mRNA cleavage, thus we cannot rule out that this target might be incorrect and regulation may be via a non-cleavage mechanism, and/or this miRNA might have other as yet unknown targets.

Expression of Potential Target Genes

The expression of miRNAs' targets was quantified by qRT-PCR with the expectation that the target's expression would be inversely correlated with expression of the miRNA. We found two miRNAs, miR169b and miR1432, that were differentially expressed under drought in at least two genotypes; hence we selected *NFY-A* and an EF-hand encoding transcript, the targets of miR169b and miR1432 respectively, for expression analysis. Expression of *NFY-A* was downregulated in all four genotypes under drought (Fig. 4a), although miR169b was only significantly induced in two genotypes, Hindmarsh and WI4304 (Fig. 2a). The mRNA transcript encoding a Calmodulin-related (EF hand containing) calcium sensor protein showed an inverse correlation with miR1432 in the cv. Hindmarsh. However, we did not observe the inverse correlation of miR1432 and this target transcript in the other three

genotypes (Fig. 4b), although we identified the ideal alignment of the canonical cleavage products with this transcript in one of our degradome libraries (Fig 3b).

This observation led us to investigate the sequence of miR1432 binding site within the target transcript in the four genotypes, which revealed that in Commander, Fleet, and WI4304, there was a G:U pair at position 12 nt, relative to the 5'-end of the miRNA of the miRNA: target duplex. However, in the genotype Hindmarsh, the sequence of miR1432 binding site within the target transcript had perfect complementarity with miR1432 and expression of the gene and miRNA were inversely correlated (Supporting Information Fig. S7).

Spatial accumulation of mature miRNAs and their targets by *in situ* –RT-PCR (ISRT-PCR)

The spatial distribution of miRNAs and target co-localization were assessed by *in situ* labelling and microscopy. We selected miR169b and miR1432 and their targets for this study since these two miRNAs were differentially expressed under drought in at least two barley genotypes. Drought-treated and well-watered Hindmarsh flag leaf samples from booting stage were used for ISRT-PCR. As expected, higher accumulation of miR169b was observed in the drought-stressed leaf compared to the well-watered leaf (Fig. 5). Inversely, *NFY-A* showed lower accumulation in the drought treated compared to the well-watered sample (Fig. 5). This inverse correlation of miR169b and *NFY-A* was observed in the mesophyll tissues (Fig. 5).

Weak accumulation of miR1432 was observed under drought compared to the well-watered sample (Fig. 6); while the target of miR1432, the EF-hand encoding transcript, showed higher accumulation in the drought treated compared with the well-watered sample (Fig. 6). miR1432 and its target were also located in mesophyll tissues (Fig. 6). The *in situ* expression

results for miR169b and miR1432 and the respective targets were consistent with our qRT-PCR results (Fig. 2 & 4).

DISCUSSION

Although miRNAs have diverse functions, and the regulatory roles of miRNAs are still not well understood, miRNA-based gene regulation has been implicated in several physiological pathways including drought stress response. In this study, the expression of eleven miRNAs in drought-stressed leaves was evaluated in four barley genotypes, Commander, Fleet, Hindmarsh and WI4304. Hindmarsh had a higher leaf water content under drought (and also in well-watered conditions) as compared to the other three genotypes (Fig. 1). Though all four genotypes are known to perform well in dry areas in Australia, these differences of water status among the genotypes may indicate greater water loss or reduced water uptake and higher stress levels during experimental drought treatment in the leaves of Commander, Fleet and WI4304 than in Hindmarsh.

Some of the miRNAs examined in our study showed different expression patterns compared to recent studies conducted in barley (Kantar *et al*., 2010; Hackenberg *et al.*, 2015). *Hv*-miR166 was more abundant under drought in barley leaves of Bűlbűl-89 (Kantar *et al*., 2010), Golden Promise and WI4330 (Hackenberg *et al*., 2015). In contrast, we found this miRNA was down under drought in one genotype, Commander, and was unchanged in the other three. Kantar *et al*. (2010) also found *Hv*-miR171 was upregulated in Bűlbűl-89 under drought stress, whereas it was not differentially abundant with drought in any of the genotypes we assayed. Hackenberg *et al*. (2015) found that homologous *Osa*-miR393a was down-regulated by drought in Golden Promise. However, we observed no significant differences in expression of this miRNA between the two watering conditions in any of our experimental genotypes (Fig. 2).

Differential expression of miRNAs has been observed between sensitive and tolerant genotypes of cowpea (Barrera-Figueroa *et al*., 2011), rice (Cheah *et al*., 2015) and durum wheat (Liu *et al*., 2015) under water deficit stress where, similarly, a small number of different genotypes was studied. The distinct behaviour of miRNAs reflected the variation in response to water limitation in these species; however we observed genotype-specific miRNA responses to water limitation in four barley genotypes with similar drought tolerance in terms of yield performance in field trials. A miRNA and its target mRNA need to be co-expressed in order for the miRNA to suppress the expression of its biological target (Kuhn *et al*., 2008). The target mRNA encoding a calmodulin related calcium sensor protein, here, showed an inverse expression pattern compared to the miR1432 under drought in only one barley genotype, Hindmarsh. We observed perfect complementarity between the miRNA: target duplex in the genotype Hindmarsh (Supporting Information Fig. S7), while there was a polymorphism in the DNA sequence of the other three genotypes which could explain the lack of complementarity and correlated expression of the miRNA: mRNA in these cultivars. This finding confirmed that miRNA-mediated target regulation varied between genotypes and suggested that this depended on miRNA: mRNA sequence-specific binding. Although some, single miRNA mediated mRNA cleavage products were aligned ideally with separate target sequences in degradome libraries from two different genotypes, Golden Promise and Pallas (Table 2), for others (for *Osa*-miR1432, *Hv*-miR166b/c and *Hv*-miR5048a) the cleavage products were only obtained in Golden Promise, but not in Pallas, again suggesting genotype-specific target binding was important for miRNA-mediated regulation.

Nonetheless, we observed that the same transcript encoding NFY-A could be the target of both *Ath*-miR169b and *Osa*-miR169n in barley, although these two miRNAs differ at four nucleotides. Our result indicated that this target could still be cleaved by these miRNAs despite seed region mismatches (Fig. 3a and Supporting Information Fig. S6e). It

has been suggested that there is the possibility of mismatch between the miRNA and the target in the seed region and, although seed region mismatches are uncommon, imperfect seed region pairing can be overcome by 3′ compensatory pairing (Witkos *et al*., 2011). The compensatory pairing in the 3′ of miRNA could reduce the seed pairing requirement to as little as four base pairs (Brennecke *et al.*, 2005; Künne *et al.*, 2014).

We found inversely correlated expression between *Ath*-miR169b and *NFY-A* (Fig. 2a & 4a) which was consistent with previous studies (Zhao *et al*. 2011; Li *et al*., 2008). We observed up-regulation of *Ath*-miR169b in Hindmarsh and WI4304 under drought (Fig. 2a) and *NFY-A* was down-regulated in all four barley genotypes under drought (Fig. 4a) so that the miRNA seed region match appeared to be less important than the genotypic target sequence for miRNA-mediated cleavage, at least at this target. Nuclear factor Y (NFY), a CCAAT box-binding transcription factor, is composed of three subunits: NFY-A, NFY-B, and NFY-C (Baxevanis *et al*., 1995). NFY family members are reported to play roles in the molecular control of flowering, seed development, photosynthesis and improved tolerance to abiotic stresses such as drought (Qu *et al*., 2015; references therein). Although *Ath*-miR169b and *NFY-A* expression were inversely correlated in two genotypes under drought, there was no correlation with the abundance of *Osa*-miR169n that could also cleave NFY-A transcripts and no significant up-regulation of *Ath*-miR169b under drought in two of four genotypes. This suggested that *NFY-A* down-regulation under drought was mediated by multiple mechanisms including miR169b mediation. In Hindmarsh under drought conditions, both the up-regulated (miR169b) and down regulated (miR1432) mature miRNAs were observed in the mesophyll cells (Figs. 5&6). As expected the NFY-A and the calmodulin related calcium sensor transcripts were also found preferentially in the same cellular compartment in leaf tissue showing inverse expression compared with their regulatory miRNAs under drought (Figs. 5&6). Information on the tissue localization of barley drought responsive miRNAs has

not been reported previously. The differential expression of these miRNAs in the mesophyll cells under drought could provide useful information for further elucidating the role of these miRNAs under stress.

miRNAs that are down-regulated under drought are expected to have targets that are positive regulators of stress responses (Wei *et al*., 2009). In our study, miR1432 was significantly down under drought in three genotypes (Fig. 2b). miR1432 was previously predicted to target the mRNAs of genes encoding EF-hand proteins in rice (Sunkar, 2008). In our degradome library, we found miR1432 mediated cleavage products ideally aligned with the target transcript encoding a calmodulin related calcium sensor protein which has EF-hand domains, and the target cleavage occurring in the canonical cleavage site (Fig. 3b). EF-hand domains contain a helix-loop-helix structural motif reported to bind with calcium (Ca^{2+}) (Cheng *et al.*, 2002). It appears that miR1432 targets EF-hand domain containing transcripts and thus indirectly contributes to calcium signalling, a vital signalling mechanism involved in various physiological processes in plants (Ni *et al.* 2009). In our study, down-regulation of miR1432 under drought appeared to mediate increased expression of its target transcript localized in mesophyll cells (Fig. 6). However, we observed up-regulation of this target transcript under drought only in Hindmarsh and not in the other three genotypes (Fig 4b) underlining the importance of functional experimentation, rather than correlative studies, with both miRNAs and their targets for understanding their roles in regulation.

Despite the majority of cleavage products here being ideally derived from canonical cleavage, for the miR444b target, a MADS-box family gene conserved in monocots (Sunkar *et al.*, 2005), we observed that target cleavage might occur between the 19^{th} and 20^{th} nt position (opposite to the miRNA) in both Golden Promise and Pallas (Supporting Information Fig. S6j). This suggested that miRNA-mediated cleavage sites might not be limited to the 10–11 nt position. The possibility of non-canonical cleavage was previously suggested by

Hackenberg *et al.* (2015). However we were unable to find any other studies that showed target cleavage at the 19th and 20th nt position. MADS-box family mRNAs were reported to be targeted by miR444b in rice where the cleavage products were obtained from the canonical cleavage site (Sunkar *et al.*, 2005). Our results demonstrated that, although numerous targets were predicted for the examined drought responsive miRNAs, only a few were regulated by miRNA mediated cleavage and these were genotype-specific. Target recognition also appeared to be genotype-specific and miRNA mediated cleavage sites varied within the miRNA: target binding region in barley.

In this study, we examined the expression of eleven miRNAs, nine of which were previously reported to be drought responsive, in four barley genotypes adapted to low-rainfall environments. Only four of 11 studied miRNAs had significant expression differences under drought in barley, and of these only two miRNAs, miR169b and miR1432, had a consistent expression pattern in more than one genotype. Bioinformatic analysis predicted numerous targets of the candidate miRNAs. Although bioinformatic analysis has been widely used for the discovery of miRNAs and prediction of targets in recent years, there is little information available on the expression of mature candidate miRNAs and biological validation of their targets. The present study provides an important glimpse into miRNA expression, target prediction and validation and the difficulty of relying on bioinformatic predictions. Localisation of miRNAs and their targets may help improve our understanding of the involvement of miRNAs in plant drought stress responses. Though drought tolerance is a complex trait, miRNA mediated differential expression of target genes that are positive regulators of stress responses could help us to identify potential biomarkers in different genotypes under drought that would be of interest for research. Additional evidence will be required to confirm miRNA-based regulation of important genes in drought stress-responsive

networks and the genotype specificity of the regulation. However, we have identified useful targets for the additional studies and evidence for genotypic variation.

ACKNOWLEDGEMENTS

Our grateful thanks to Dr. Bu-Jun Shi for initiating the project; Dr. Gwenda M Mayo and Dr. Takashi Okada for supporting tissue fixation, embedding and sectioning; Asmini Athman for training for the *in situ* PCR; Yuan Li and Hui Zhou for performing the qRT-PCR; Janine Jones for some statistical analysis; and Dr. Runxuan Zhang for early discussion about miRNA target prediction.

REFERENCES

Alam M.M., Tanaka T., Nakamura H., Ichikawa H., Kobayashi K., Yaeno T.,…, Nishiguchi M. (2015) Overexpression of a rice heme activator protein gene (*OsHAP2E*) confers resistance to pathogens, salinity and drought, and increases photosynthesis and tiller number. *Plant Biotechnology Journal* **13**, 85–96.

Athman A., Tanz S.K., Conn V., Jordans C., Mayo G.M., Ng W.W., …, Gilliham M. (2014) Protocol: A fast and simple *in situ* PCR method for localising gene expression in plant tissue. *Plant Methods* **10**, 29-47.

Bagasra O. (2007) Protocols for the *in situ* PCR-amplification and detection of mRNA and DNA sequences. *Nature Protocols* **2**, 2782–2795.

Balcells I., Cirera S. & Busk P.K. (2011) Specific and sensitive quantitative RT-PCR of miRNAs with DNA primers. *BMC Biotechnology* **11**, 70-81.

Barrera-Figueroa B.E., Gao L., Diop N.N., Wu Z., Ehlers J.D., Roberts P.A., …, Liu R. (2011) Identification and comparative analysis of drought-associated microRNAs in two cowpea genotypes. *BMC Plant Biology* **11**, 127.

Barrs H.D. & Weatherley P.E. (1962) A re-examination of the relative turgidity technique for estimating water deficit in leaves. *Australian Journal of Biological Sciences* **15**, 413-428.

Bartel D.P. (2004) MicroRNAs: Genomics, Biogenesis, Mechanism, and Function. *Cell* **116**, 281-297.

Baumberger N. & Baulcombe D.C. (2005) *Arabidopsis* ARGONAUTE1 is an RNA slicer that selectively recruits microRNAs and short interfering RNAs. *Proceedings of the National Academy of Sciences of the United States of America* **102**, 3691–3696.

Baxevanis A.D, Arents G., Moudrianakis E.N. & Landsman D. (1995) A variety of DNA-binding and multimeric proteins contain the histone fold motif. *Nucleic Acids Research* **23**, 2685–2691.

Benes V. & Castoldi M. (2010) Expression profiling of microRNA using real-time quantitative PCR, how to use it and what is available. *Methods* **50**, 244–249.

Berger Y., Harpaz-Saad S., Brand A., Melnik H., Sirding N., Alvarez J.P., Zinder M., Samach A., Eshed Y. & Ori N. (2009) The NAC-domain transcription factor GOBLET specifies leaflet boundaries in compound tomato leaves. *Development* **136**, 823–832.

Boyer J.S. (1967) Leaf water potentials measured with a pressure chamber. *Plant Physiology* **42**, 133–137.

Brennecke J., Stark A., Russell R.B. & Cohen S.M. (2005) Principles of microRNA-target recognition. *PLoS Biology* **3**, e85.

Budak H., Kantar M., Bulut R. & Akpinar B.A. (2015) Stress responsive miRNAs and isomiRs in cereals. *Plant Science* **235,** 1–13.

Camacho C., Coulouris G., Avagyan V., Ma N., Papadopoulos J., Bealer K., & Madden T.L. (2009) BLAST+: architecture and applications. *BMC Bioinformatics* **10**, 421-429.

Cheah B.H., Nadarajah K., Divate M.D. & Wickneswari R. (2015) Identification of four functionally important microRNA families with contrasting differential expression profiles between drought-tolerant and susceptible rice leaf at vegetative stage. *BMC Genomics* **16**, 692-709.

Chen C., Ridzon D.A., Broomer A.J., Zhou Z., Lee D.H., Nguyen J.T.,,…, Guegler K.J. (2005) Real-time quantification of microRNAs by stem-loop RT-PCR. *Nucleic Acids Research* **33**, e179.

Cheng S.H., Willmann M.R., Chen H.C. & Sheen J. (2002) Calcium Signaling through Protein Kinases. The Arabidopsis Calcium-Dependent Protein Kinase Gene Family. *Plant Physiology* **129**, 469-485.

Coventry S., Davis L., Fleury D. & Eglinton J. (2012) Barley breeding for low rainfall Environments. *Eyre Peninsula Farming Systems 2012 Summary*. http://eparf.com.au/wp-content/uploads/2014/11/2012-18.-Barley-breeding-for-low-rainfall-environments-.pdf.

Dehury B., Panda D., Sahu J., Sahu M., Sarma K., Barooah M., Sen P., & Modi M.K. (2013) In silico identification and characterization of conserved miRNAs and their target genes in sweet potato (*Ipomoea batatas* L.) Expressed Sequence Tags (ESTs). *Plant Signaling and Behavior* **8**, e26543.

Ferdous J., Hussain S.S. & Shi B.J. (2015a) Role of microRNAs in plant drought tolerance. *Plant Biotechnology Journal* **13**, 293–305.

Ferdous J., Li Y., Reid N., Langridge P., Shi B.J. & Tricker P.J. (2015b) Identification of Reference Genes for Quantitative Expression Analysis of MicroRNAs and mRNAs in Barley under Various Stress Conditions. *PLoS ONE* **10**, e0118503.

Fettell N. (2011) BARLEY VARIETIES AND AGRONOMY UPDATE 2011. http://riverineplains.com.au/_literature_85465/Barley_varieties_and_agronomy_update_-_Neil_Fettell.

Gu S. & Kay M.A. (2010) How do miRNAs mediate translational repression? *Science* **1**, 11-15.

Gutierrez L., Bussell J.D., Păcurar D.I., Schwambach J., Păcurar M. & Bellinia C. (2009) Phenotypic plasticity of adventitious rooting in *Arabidopsis* is controlled by complex regulation of AUXIN RESPONSE FACTOR transcripts and microRNA abundance. *The Plant Cell* **21**, 3119–3132.

Hackenberg M., Gustafson P., Langridge P. & Shi B.J. (2015) Differential expression of microRNAs and other small RNAs in barley between water and drought conditions. *Plant Biotechnology Journal* **13**, 2–13.

Hackenberg M., Huang P.J., Huang C.Y., Shi B.J., Gustafson P. & Langridge P. (2013) A comprehensive expression profile of microRNAs and other classes of non-coding small RNAs in barley under phosphorous-deficient and -sufficient conditions. *DNA Research* **20**, 109–125.

Hackenberg M., Shi B.J., Gustafson P. & Langridge P. (2012) A Transgenic Transcription Factor (TaDREB3) in Barley Affects the Expression of MicroRNAs and Other Small Non-Coding RNAs. *PLoS ONE* **7**: e42030.

Huntzinger E. & Izaurralde E. (2011) Gene silencing by microRNAs: contributions of translational repression and mRNA decay. *Nature Reviews Genetics* **12**, 99–110.

Jones-Rhoades M.W., Bartel D.P. & Bartel B. (2006) MicroRNAS and their regulatory roles in plants. *Annual Review of Plant Biology* **57**, 19-53.

Kantar M., Lucas S. & Budak H. (2011) miRNA expression patterns of *Triticum dicoccoides* in response to shock drought stress. *Planta* **233**, 471–484.

Kantar M., Unver T. & Budak H. (2010) Regulation of barley miRNAs upon dehydration stress correlated with target gene expression. *Functional and Integrative Genomics* **10**, 493–507.

Kozomara A. & Griffiths-Jones S. (2014) miRBase: annotating high confidence microRNAs using deep sequencing data. *Nucleic Acids Research* **42**, D68–D73.

Krol J., Loedige I. & Filipowicz W. (2010) The widespread regulation of microRNA biogenesis, function and decay. *Nature Reviews Genetics* **11**, 597–610.

Kuhn D.E., Martin M.M., Feldman D.S., Terry A.V., Nuovo G.J. & Elton T.S. (2008) Experimental Validation of miRNA Targets. *Methods* **44**, 47-54.

Künne T., Swarts D.C. & Brouns S.J. (2014) Planting the seed: target recognition of short guide RNAs. *Trends in Microbiology* **22**, 74–83.

Langridge P. & Reynolds M. (2015) Genomic tools to assist breeding for drought tolerance. *Current Opinion Biotech* **32**, 130-135.

Lee R.C., Feinbaum R.L. & Ambros V. (1993) The *C-elegans* heterochronic gene *LIN-4* encodes small RNAs with antisense complementarity to *LIN-14*. *Cell* **75**, 843-854.

Leyva-Gonzalez M.A., Ibarra-Laclette E., Cruz-Ramırez A. & Herrera-Estrella L. (2012) Functional and transcriptome analysis reveals an acclimatization strategy for abiotic stress tolerance mediated by *Arabidopsis* NF-YA family members. *PLoS ONE* **7**, e48138.

Liu H., Searle I.R., Watson-Haigh N.S., Baumann U., Mather D.E., Able A.J. & Able J.A (2015) Genome-Wide Identification of MicroRNAs in Leaves and the Developing

Head of Four Durum Genotypes during Water Deficit Stress. *PLoS ONE* **10**, e0142799.

Li W.X., Oono Y., Zhu J., He X.J., Wu J.M., Iida K.,…, Zhu J.K. (2008) The *Arabidopsis* NFYA5 transcription factor is regulated transcriptionally and posttranscriptionally to promote drought resistance. *The Plant Cell* **20**, 2238–2251.

Li X., Ni M., Zhang C., Ma W. & Zhang Y. (2014). A convenient system for highly specific and sensitive detection of miRNA expression. *RNA* **20**, 252–259.

Lu S.F., Sun Y.H., Shi R., Clark C., Li L.G. & Chiang V.L. (2005) Novel and mechanical stress-responsive microRNAs in *Populus trichocarpa* that are absent from *Arabidopsis*. *The Plant Cell* **17**, 2186–2203.

Møller I.S., Gilliham M., Jha D., Mayo G.M., Roy S.J., Coates J.C.,..., Tester M. (2009) Shoot Na+ exclusion and increased salinity tolerance engineered by cell type-specific alteration of Na+ transport in *Arabidopsis*. *The Plant Cell* **21**, 2163–2178.

Ni F.T., Chu L.Y., Shao H.B. & Liu Z.H. (2009) Gene expression and regulation of higher plants under soil water stress. *Current Genomics* **10**, 269–280.

Ni Z., Hu Z., Jiang Q. & Zhang H. (2013) *GmNFYA3*, a target gene of miR169, is a positive regulator of plant tolerance to drought stress. *Plant Molecular Biology* **82**, 113– 129.

Przybecki Z., Siedlecka E., Filipecki M. & Urbańczyk-Wochniak E. (2006) *In situ* reverse transcription PCR on plant tissues. *Methods in Molecular Biology* **334**,181–197.

Qu B., He X., Wang J., Zhao Y., Teng W., Shao A.,…, Tong Y. (2015) A wheat CCAAT box-binding transcription factor increases the grain yield of wheat with less fertilizer input. *Plant Physiology* **167**, 411–423.

Reinhart B.J., Weinstein E.G., Rhoades M.W., Bartel B. & Bartel D.P. (2002) MicroRNAs in plants. *Genes and Development* **16**, 1616-1626.

Robinson J.T., Thorvaldsdóttir H., Winckler W., Guttman M., Lander E.S., Getz G. & Mesirov J.P. (2011) Integrative Genomics Viewer. *Nature Biotechnology* **29**, 24–26.

Schreiber A., Shi B.J., Huang C.Y., Langridge P. & Baumann U. (2011) Discovery of barley miRNAs through deep sequencing of short reads. *BMC Genomics* **12**, 129-149.

Shen D., Suhrkamp I., Wang Y., Liu S., Menkhaus J., Verreet J.A., Fan L. & Cai D. (2014) Identification and characterization of microRNAs in oilseed rape (*Brassica napus*) responsive to infection with the pathogenic fungus *Verticillium longisporum* using *Brassica* AA (*Brassica rapa*) and CC (*Brassica-oleracea*) as reference genomes. *New Phytologist* **204**, 577-594.

Sunkar R., Girke T., Jain P.K. & Zhu J.K. (2005) Cloning and characterization of microRNAs from rice. *The Plant Cell* **17**, 1397–411.

Sunkar R., Zhou X., Zheng Y., Zhang W. & Zhu J.K. (2008) Identification of novel and candidate miRNAs in rice by high throughput sequencing. *BMC Plant Biology* **8**, 25-41.

Trindade I., Capitao C., Dalmay T., Fevereiro M.P. & dos Santos D.M. (2010) miR398 and miR408 are up-regulated in response to water deficit in *Medicago truncatula*. *Planta* **231**, 705–716.

Varkonyi-Gasic E., Wu R., Wood M., Walton E.F. & Hellens R.P. (2007) Protocol: a highly sensitive RT-PCR method for detection and quantification of microRNAs. *Plant Methods* **3**, 12-23.

Vazquez F., Legrand S. & Windels D. (2010) The biosynthetic pathways and biological scopes of plant small RNAs. *Trends in Plant Science* **15**, 337–345.

Wang T., Chen L., Zhao M., Tian Q. & Zhang W.H. (2011) Identification of drought-responsive microRNAs in *Medicago truncatula* by genome-wide high-throughput sequencing. *BMC Genomics* **12**, 1–11.

Wei L., Zhang D., Xiang F. & Zhang Z. (2009) Differentially expressed miRNAs potentially involved in the regulation of defense mechanism to drought stress in maize seedlings. *International Journal of Plant Sciences* **170**, 979-989.

Witkos T., Koscianska E., & Krzyzosiak W. (2011) Practical Aspects of microRNA Target Prediction. *Current Molecular Medicine* **11**, 93–109.

Xie F. & Zhang B. (2010) Target-align: a tool for plant microRNA target identification. *Bioinformatics* **26**, 3002–3003.

Zhang B.H., Pan X.P., Wang Q., Cobb G.P. & Anderson T.A. (2006) Computational identification of microRNAs and their targets. *Computational Biology and Chemistry* **30**, 395–407.

Zhang X., Zou Z., Gong P., Zhang J., Ziaf K., Li H., Xiao F. & Ye Z. (2011) Over-expression of microRNA169 confers enhanced drought tolerance to tomato. *Biotechnology Letters* **33**, 403–9.

Zhao M., Ding H., Zhu J.K., Zhang F. & Li W.X. (2011) Involvement of miR169 in the nitrogen-starvation responses in Arabidopsis. *New Phytologist* **190**, 906–915.

Zhou L., Liu Y., Liu Z., Kong D., Duan M. & Luo, L. (2010) Genome-wide identification and analysis of drought-responsive microRNAs in *Oryza sativa*. *Journal of Experimental Botany* **61**, 4157–4168.

Zhu J.K. (2002) Salt and drought stress signal transduction in plants. *Annual Review of Plant Biology* **53**, 247-273.

Table 1. Primers used for the miRNA stem-loop qRT-PCR

miRNA sequence	miRNA sequence	Primer (5′–3′)	miRBase Accession number
Hv-miR166b/c	UCGGACCAGGCUUCAUUCC	Stem-loopRT GTCGTATCCAGTGCAGGGAGGGAGGTATTCGCACTGGATACGACGGAATG Forward AATGTTCCTTCGGACCAGG Modified Reverse GTGCAGGGAGGGAGGT	MIMAT0020737
Ath-miR169b	CAGCCAAGGAUGACUUGCCGG	Stem-loopRT GTCGTATCCAGTGCAGGGTCCGAGGTATTCGCACTGGATACGACCCGGCA Forward TACACGGCAGCCAAGGATGAC Universal Reverse GTGCAGGGTCCGAGGT	MIMAT0000906
Osa-miR169n	UAGCCAAGAAUGACUUGCCUA	Stem-loopRT GTCGTATCCAGTGCAGGGTCCGAGGTATTCGCACTGGATACGACTAGGCA Forward GCGTGCTGTAGCCAAGAATGAC Universal Reverse GTGCAGGGTCCGAGGT	MIMAT0001059
Hv-miR171	UGUUGGCUCGACUCACUCAGA	Stem-loopRT GTCGTATCCAGTGCAGGGAGGGAGGTATTCGCACTGGATACGACTCTGAG Forward CTGCTACTGTGTTGGCTCGACTC Modified Reverse GTGCAGGGAGGGAGGT	MIMAT0022971
Osa-miR393a	UCCAAAGGGAUCGCAUUGAUC	Stem-loopRT GTCGTATCCAGTGCAGGGTCCGAGGTATTCGCACTGGATACGACGATCAA Forward ACTATGCTCCAAAGGGATCGC Universal Reverse GTGCAGGGTCCGAGGT	MIMAT0000957
Bdi-miR396b	UCCACAGGCUUUCUUGAACUG	Stem-loopRT GTCGTATCCAGTGCAGGGTCCGAGGTATTCGCACTGGATACGACACAGTTC Forward TTGTCAGTCCACAGGCTTTCT Universal Reverse GTGCAGGGTCCGAGGT	MIMAT0020700
Hv-miR444b	UGCAGUUGCUGUCUCAAGCUU	Stem-loopRT GTCGTATCCAGAGCTGGGTCCGAGGTATTCGCTCTGGATACGACAAGCTT Forward TCGTTCAGTTGCAGTTGCTGTC Modified reverse-2 GAGCTGGGTCCGAGGT	MIMAT0020543
Osa-miR1432	AUCAGGAGAGAUGACACCGAC	Stem-loopRT GTCGTATCCAGTGCAGGGTCCGAGGTATTCGCACTGGATACGACGTCGGT	MIMAT0005966

		Forward GGTGTGGCATCAGGAGAGATG Universal Reverse GTGCAGGGTCCGAGGT	
Hv-miR5048a	UAUUUGCAGGUUUUAGGUCUAA	Stem-loopRT GTCGTATCCAGTGCAGGGAGGGAGGTATTCGCACTGGATACGACTTAGAC Forward CGTCTTCGGTATTTGCAGGTTTTA Modified Reverse GTGCAGGGAGGGAGGT	MIMAT0020544
Ata-miR9863a	UGAGAAGGUAGAUCAUAAUAGC	Stem-loopRT GTCGTATCCAGTGCAGGGAGGGAGGTATTCGCACTGGATACGACGCTATT Forward TCGGCGGTGAGAAGGTAGATCA Modified Reverse GTGCAGGGAGGGAGGT	MIMAT0037104
Hv-miRx5	ACUGGUUGGAUCAUGCUUCUC	Stem-loopRT GTCGTATCCAGTGCAGGGAGGGAGGTATTCGCACTGGATACGACGAGAAG Forward primer TTGCGACTGGTTGGATCAT Modified Reverse GTGCAGGGAGGGAGGT	-

Table 2. miRNA targets confirmed through degradome analysis

Homologous miRNAs	Targets functions	MLOC numbers	Contig number (from JHI Database Barley WGS Morex Assembly v3)	Genbank accession
Hv-miR166b/c	Homeobox domain (HD)- START domain containing protein	MLOC_58644	contig_42852	AK359910.1
	HD-START domain, MEKHLA domain containing protein	MLOC_79063	contig_8318	AK365312.1
	HD-START domain, MEKHLA domain containing protein	MLOC_33978	contig_241849	AK364215.1
	HD-START domain, MEKHLA domain containing protein	MLOC_61603	contig_45665	AK362009.1
Ath-miR169b	CCAAT-binding transcription factor (CBF-B/NF-YA) subunit	MLOC_36554	contig_2546965	AK368372.1
Osa-miR169n	CCAAT-binding transcription factor (CBF-B/NF-YA) subunit	MLOC_36554	contig_2546965	AK368372.1
Osa-miR393a	Leucine-rich repeat (LRR) domain containing F-box protein	MLOC_9864	contig_1557974	AK355927.1
	Leucine-rich repeat (LRR) domain containing F-box protein	MLOC_56088	contig_40541	Not available
Bdi-miR396b	WRC and QLQ domain: DNA binding and involved in mediating protein interactions respectively	MLOC_67201	contig_52709	AK376067.1
	WRC domain: DNA binding	MLOC_66132	contig_51136	AK376404.1
Hv-miR444b	MADS-box family gene with MIKCc type-box, expressed	MLOC_61033	contig_45023	AK358388.1
Osa-miR1432	Calmodulin-related calcium sensor protein (contains EF hand domain)	MLOC_70272	contig_57713	Not available
Hv-miR5048a	Serine/threonine-protein kinase receptor precursor	MLOC_70446	contig_57988	DQ469714.1
Ata-miR9863	NB-ARC domain	MLOC_24045	contig_163538	AK372887.1
	NB-ARC domain	MLOC_21626	contig_1596863	AF427791.1

Figure legends

Figure 1. Response of four barley genotypes to drought. (a) Mean leaf water potential and (b) relative water content of fully expanded, mature leaves of four barley genotypes (Commander, Fleet, Hindmarsh and WI4304) at booting stage under drought and in the well-watered control (n=12). The error bars are ±0.5 lsd. The means are significantly different when the error bars do not overlap.

Figure 2. Absolute quantification (qRT-PCR) of the number of mature candidate miRNAs; (a) *Ath*-miR169b, (b) *Osa*-miR1432, (c) *Hv*-miRx5, (d) *Hv*-miR166b/c, (e) *Osa*-miR393a, (f) *Ata*-miR9863, (g) *Bdi*-miR396b, (h) *Hv*-miR5048, (i) *Hv*-miR444b, (j) *Osa*-miR169n, (k) *Hv*-miR171 in 1µg of total RNA in flag leaves of four barley genotypes (Commander, Fleet, Hindmarsh and WI4304) at booting stage under drought and in the well-watered control (n=5). The error bars are ±0.5 lsd. The means between watering conditions are significantly different when the error bars do not overlap.

Figure 3. Validation of target transcripts encoding NFYA (JLOC1_23550/ MLOC_36554) and Calmodulin-related (EF-hand containing) calcium sensor protein (JLOC1_46633/ MLOC_70272) through degradome analysis. Degradome sequences from two barley genotypes; Golden Promise (GP) and Pallas were aligned with the candidate target transcripts. (a) NFY-A target cleavage products were obtained for both genotypes; GP and Pallas. (b) EF-hand containing target cleavage products were obtained in one genotype, GP. Positions of cleavage products are shown in the horizontal red bars. Blue bars indicate the miRNA binding site in the target transcript in 5' -3' direction. The canonical cleavage site of the target (opposite to the miRNA) is indicated between the 5' 10 and 11 nucleotide position of the miRNA. Grey bars represent the number of nucleotides matched in the alignment

between the cleavage product sequence and the reference transcript; observed mismatch is marked for the base 'c' in the red bar of (a).

Figure 4. Absolute quantification (qRT-PCR) of the number of transcripts of putative target mRNAs (a) NFY-A (target of miR169b) and (b) Calmodulin-related (EF hand containing) calcium sensor protein (target of miR1432) in 1µg of total RNA in flag leaves of four barley genotypes (Commander, Fleet, Hindmarsh and WI4304) at booting stage under drought and in the well-watered control (n=5). The error bars are ±0.5 lsd. The means between watering conditions are significantly different when the error bars do not overlap.

Figure 5. Light micrographs of the expression of *Ath*-miR169b and the target transcript encoding NFY-A by *in situ* PCR in Hindmarsh flag leaf sections from booting stage. Negative controls of miR169b are shown in (a) well-watered and (b) drought treated samples. Negative controls of NFY-A are shown in (c) well-watered and (d) drought treated samples. miR169b expression is shown in (e) well-watered and (f) drought treated samples. NFY-A expression is shown in (g) well-watered and (h) drought treated samples. Magnified view of the red boxed area of respective middle panel is shown the right panel (i-l). The blue stain indicates the presence of transcripts. Scale bar is 100µm. PH, phloem; XY, xylem; BS, bundle sheath; CO, collenchyma, MS, mesophyll cells.

Figure 6. Light micrographs of the expression of *Osa*-miR1432 and the target transcript encoding Calmodulin-related (EF hand containing) calcium sensor protein by *in situ* PCR in Hindmarsh flag leaf sections from booting stage. Negative controls of miR1432 are shown in (a) well-watered and (b) drought treated samples. Negative controls of the target transcript are shown in (c) well-watered and (d) drought treated samples. miR1432 expression is shown in (e) well-watered and (f) drought treated samples. The target transcript expression is shown in (g) well-watered and (h) drought treated samples. Magnified view of the red boxed area of respective middle panel is shown the right panel (i-l). The blue stain indicates the presence of

transcripts. Scale bar is 100μm. PH, phloem; XY, xylem; BS, bundle sheath; CO, collenchyma, MS, mesophyll cells.

Figure S1. Time to boot swollen (days from sowing) of four barley genotypes (Commander, Fleet, Hindmarsh and WI4304) under the experimental conditions. The error bars are ±0.5 lsd. The means (n=12) are significantly different when the error bars do not overlap.

Figure S2. Leaf biomass of four barley genotypes (Commander, Fleet, Hindmarsh and WI4304) under the experimental conditions. (a) Fresh weight and (b) dry weight of fully expanded, mature leaves at booting stage under drought and in the well-watered control. The error bars are ±0.5 lsd. The means (n=12) are significantly different when the error bars do not overlap.

Figure S3. Melt curve analysis of the mature miRNAs for qRT-PCR.

Figure S4. The sequencing verification of miRNA stem-loop qRT-PCR products (a-k). Reverse complementary sequence of the forward primers for respective miRNA is shown in the yellow box. M13 reverse primer was used for sequencing to verify the miRNA sequence. The nucleotide sequence which is/are not contained by the forward primer was considered as signature nucleotide(s), and verified through sequencing (indicated by red arrow in each figure).

Figure S5. Experimental design of genotypes and treatments.

a. Layout of genotypes. Black borders indicate pots. The genotypes are coded; Com = Commander, Fle = Fleet, Hin = Hindmarsh, WI4 = WI 4304. b. Layout of the watering conditions of the respective pots, Dro = Drought treated pot, Wel = Well-watered pot.

Figure S6. Degradome results for miRNA target validation (a-n). Cleavage products of two degradome libraries developed from two barley genotypes; Golden Promise (GP) and Pallas aligned with the candidate target transcripts. Some target cleavage products were

obtained either in GP (a, b, c, d, k and m) or in Pallas (l). Some target cleavage products were obtained in both genotypes (e, f, g, h, i, j). Positions of cleavage products are shown in the horizontal red bars. The blue bar indicates the miRNA binding site of the target transcript (5' -3' direction). The canonical cleavage site of the target (opposite to the miRNA) is indicated between the 5' 10 and 11 nucleotide position of the miRNA. Grey bar represents the number of nucleotides matched in the alignment between the cleavage product sequence and the reference transcript.

Figure S7. miR1432 Target site sequence of the four barley genotypes. G:U pair at the position 12 nt (from 5'-end of the miRNA) in the miRNA: target duplex in genotype (a) Commander, (b) Fleet, and (c) WI4304. (d) Perfect complementary pairing in the miRNA: target duplex in the genotype Hindmarsh.

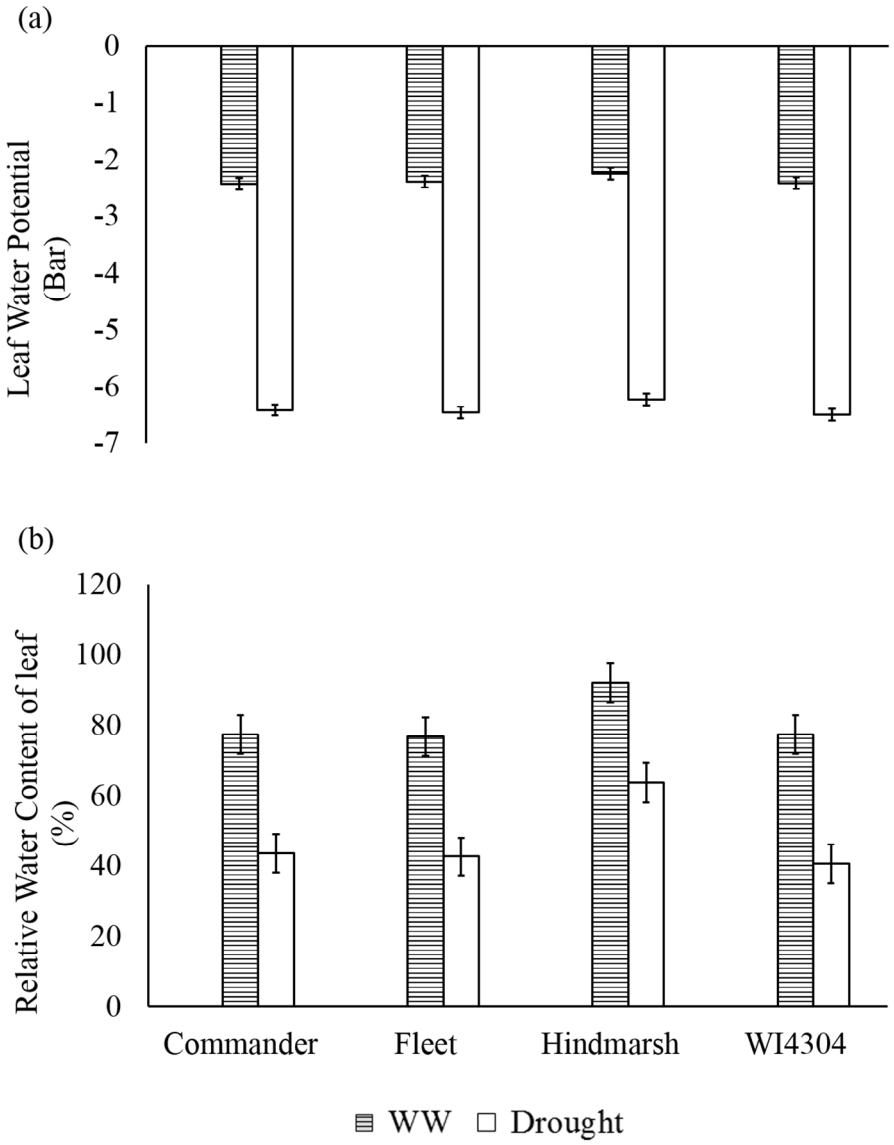

Figure 1. Response of four barley genotypes to drought. (a) Mean leaf water potential and (b) relative water content of fully expanded, mature leaves of four barley genotypes (Commander, Fleet, Hindmarsh and WI4304) at booting stage under drought and in the well-watered control (n=12). The error bars are ±0.5 lsd. The means are significantly different when the error bars do not overlap.
209x270mm (150 x 150 DPI)

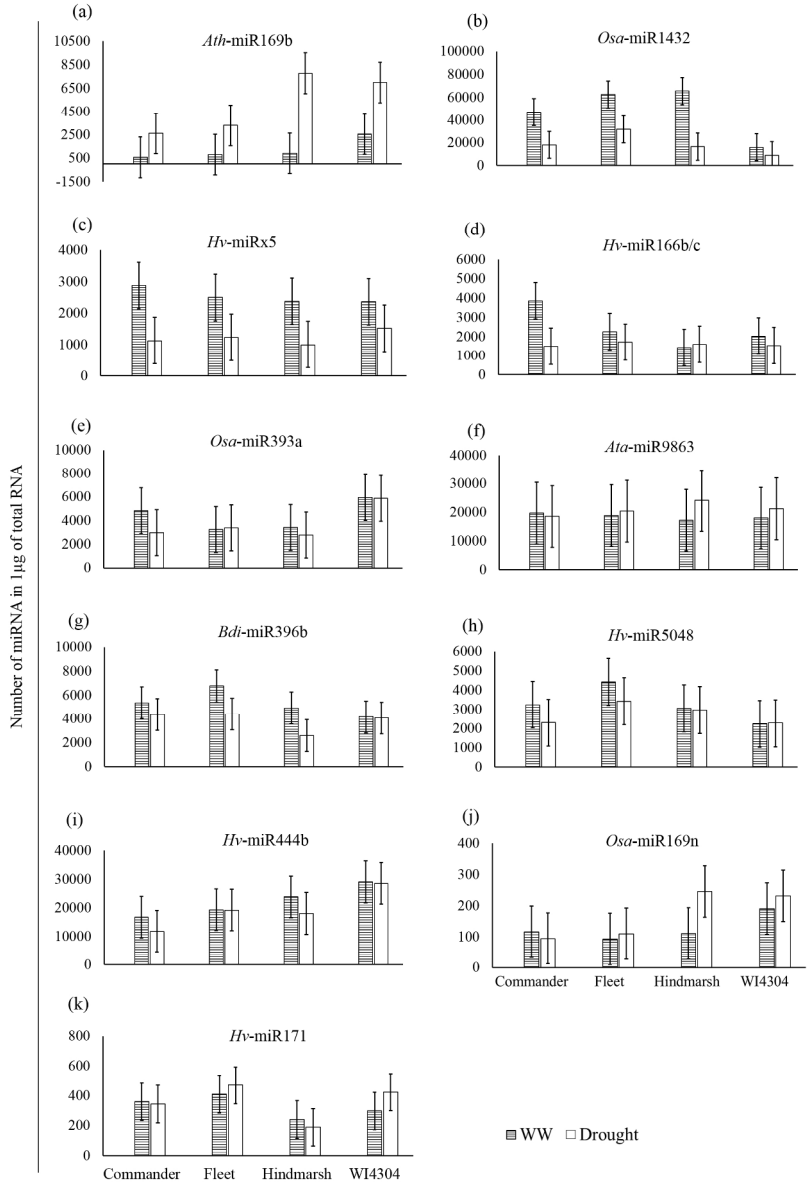

Figure 2. Absolute quantification (qRT-PCR) of the number of mature candidate miRNAs; (a) *Ath*-miR169b, (b) Osa-*miR1432, (c) Hv-miRx5, (d) Hv-miR166b/c, (e) Osa-miR393a, (f) Ata-miR9863, (g) Bdi-miR396b, (h) Hv-miR5048, (i) Hv-miR444b, (j) Osa-miR169n, (k) Hv-miR171 in 1µg of total RNA in flag leaves of four barley genotypes (Commander, Fleet, Hindmarsh and WI4304) at booting stage under drought and in the well-watered control (n=5). The error bars are ±0.5 lsd. The means between watering conditions are significantly different when the error bars do not overlap.*
349x514mm (150 x 150 DPI)

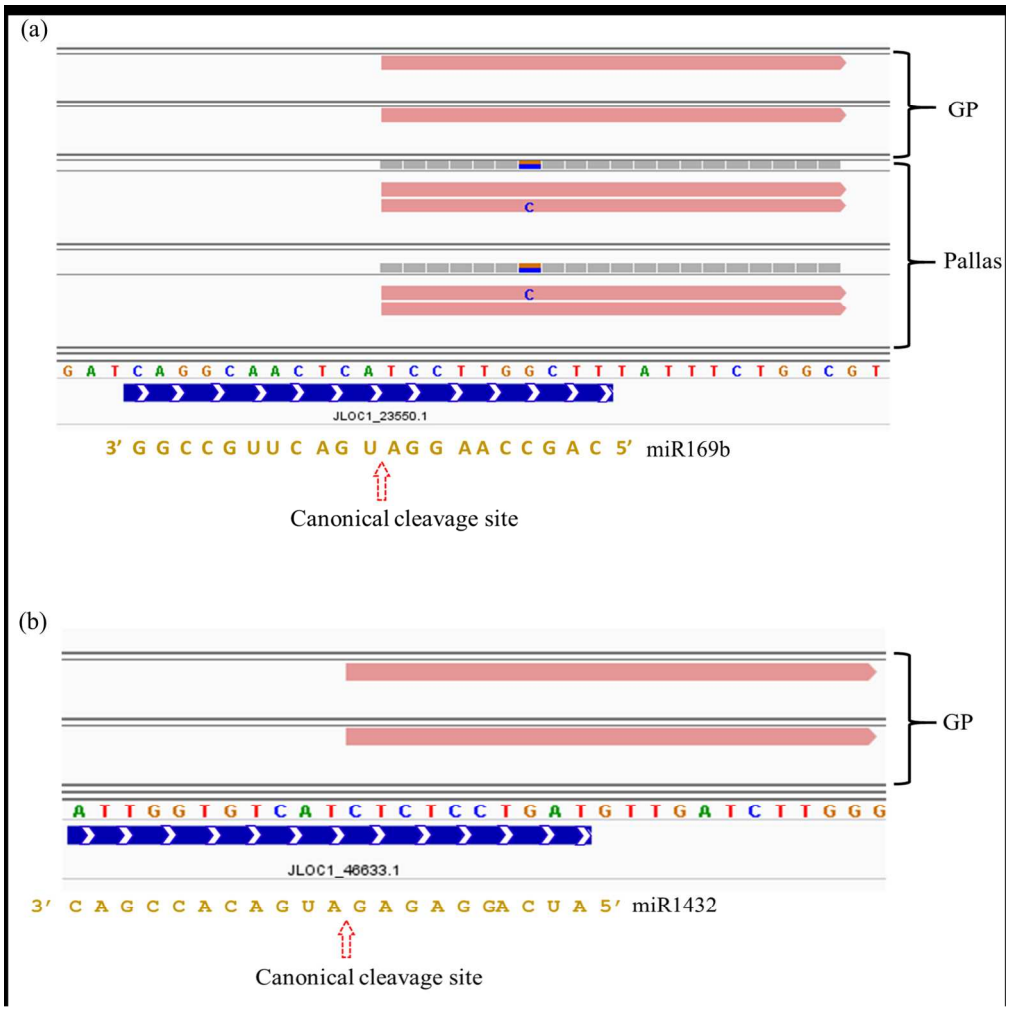

Figure 3. Validation of target transcripts encoding NFYA (JLOC1_23550/ MLOC_36554) and Calmodulin-related (EF-hand containing) calcium sensor protein (JLOC1_46633/ MLOC_70272) through degradome analysis. Degradome sequences from two barley genotypes; Golden Promise (GP) and Pallas were aligned with the candidate target transcripts. (a) NFY-A target cleavage products were obtained for both genotypes; GP and Pallas. (b) EF-hand containing target cleavage products were obtained in one genotype, GP. Positions of cleavage products are shown in the horizontal red bars. Blue bars indicate the miRNA binding site in the target transcript in 5' -3' direction. The canonical cleavage site of the target (opposite to the miRNA) is indicated between the 5' 10 and 11 nucleotide position of the miRNA. Grey bars represent the number of nucleotides matched in the alignment between the cleavage product sequence and the reference transcript; observed mismatch is marked for the base 'c' in the red bar of (a).
314x314mm (150 x 150 DPI)

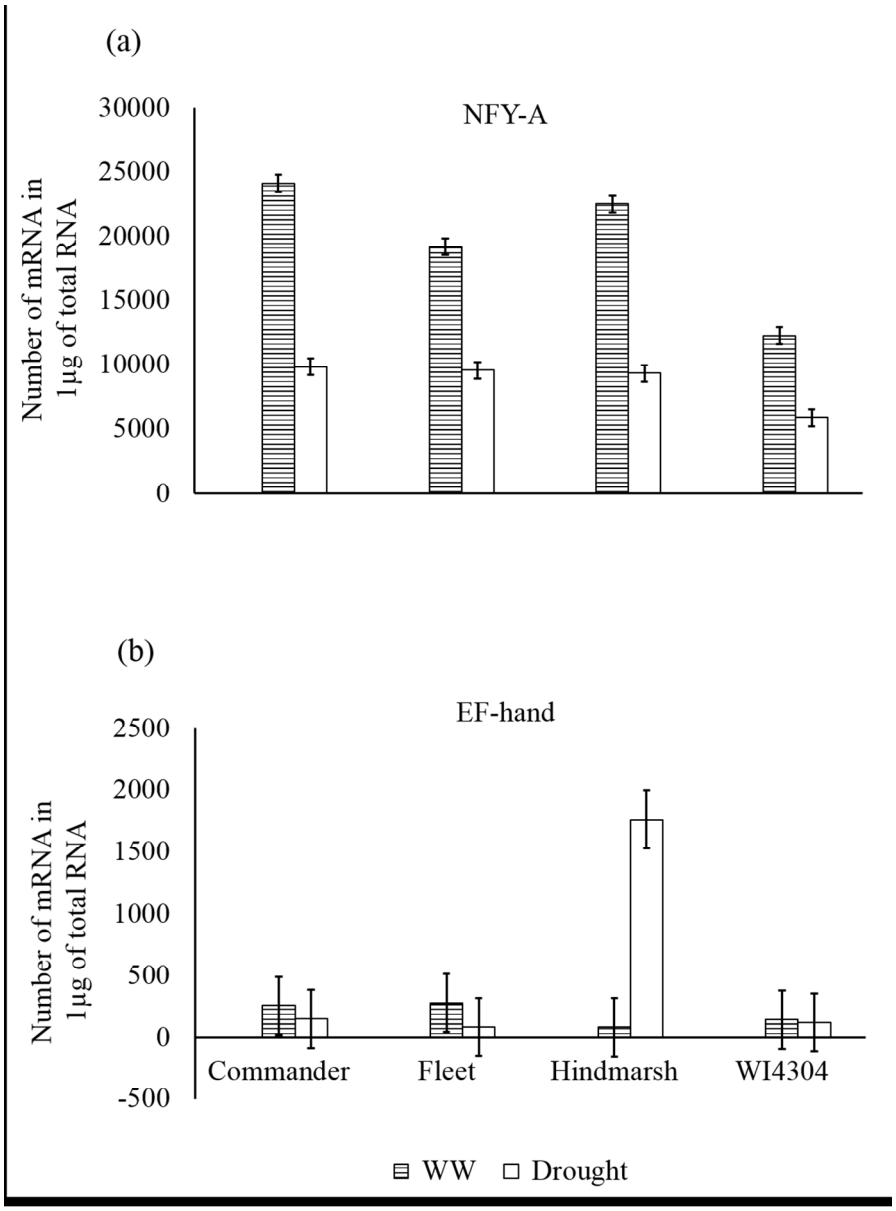

Figure 4. Absolute quantification (qRT-PCR) of the number of transcripts of putative target mRNAs (a) NFY-A (target of miR169b) and (b) Calmodulin-related (EF hand containing) calcium sensor protein (target of miR1432) in 1µg of total RNA in flag leaves of four barley genotypes (Commander, Fleet, Hindmarsh and WI4304) at booting stage under drought and in the well-watered control (n=5). The error bars are ±0.5 lsd. The means between watering conditions are significantly different when the error bars do not overlap.
195x265mm (150 x 150 DPI)

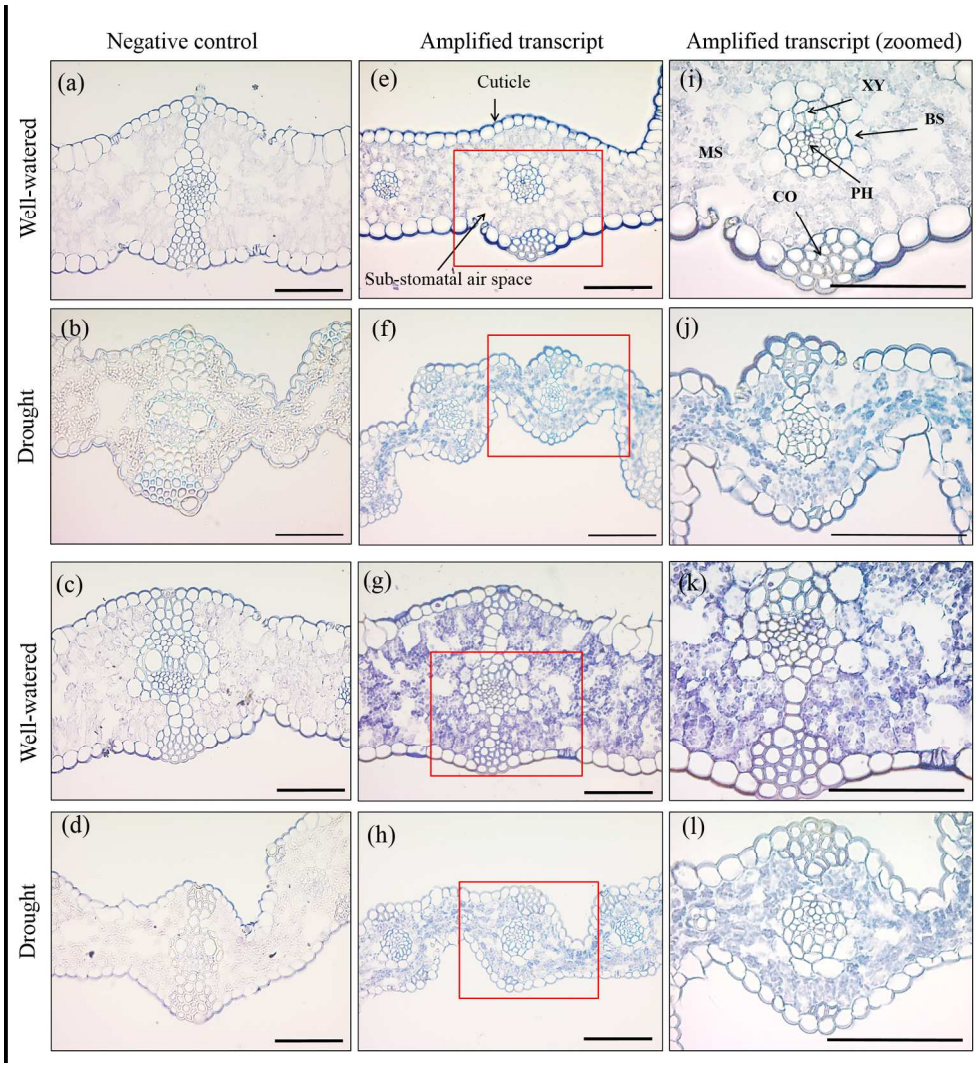

Figure 5. Light micrographs of the expression of *Ath*-miR169b and the target transcript encoding NFY-A by *in situ* PCR in Hindmarsh flag leaf sections from booting stage. Negative controls of miR169b are shown in (a) well-watered and (b) drought treated samples. Negative controls of NFY-A are shown in (c) well-watered and (d) drought treated samples. miR169b expression is shown in (e) well-watered and (f) drought treated samples. NFY-A expression is shown in (g) well-watered and (h) drought treated samples. Magnified view of the red boxed area of respective middle panel is shown the right panel (i-l). The blue stain indicates the presence of transcripts. Scale bar is 100μm. PH, phloem; XY, xylem; BS, bundle sheath; CO, collenchyma, MS, mesophyll cells.
344x363mm (150 x 150 DPI)

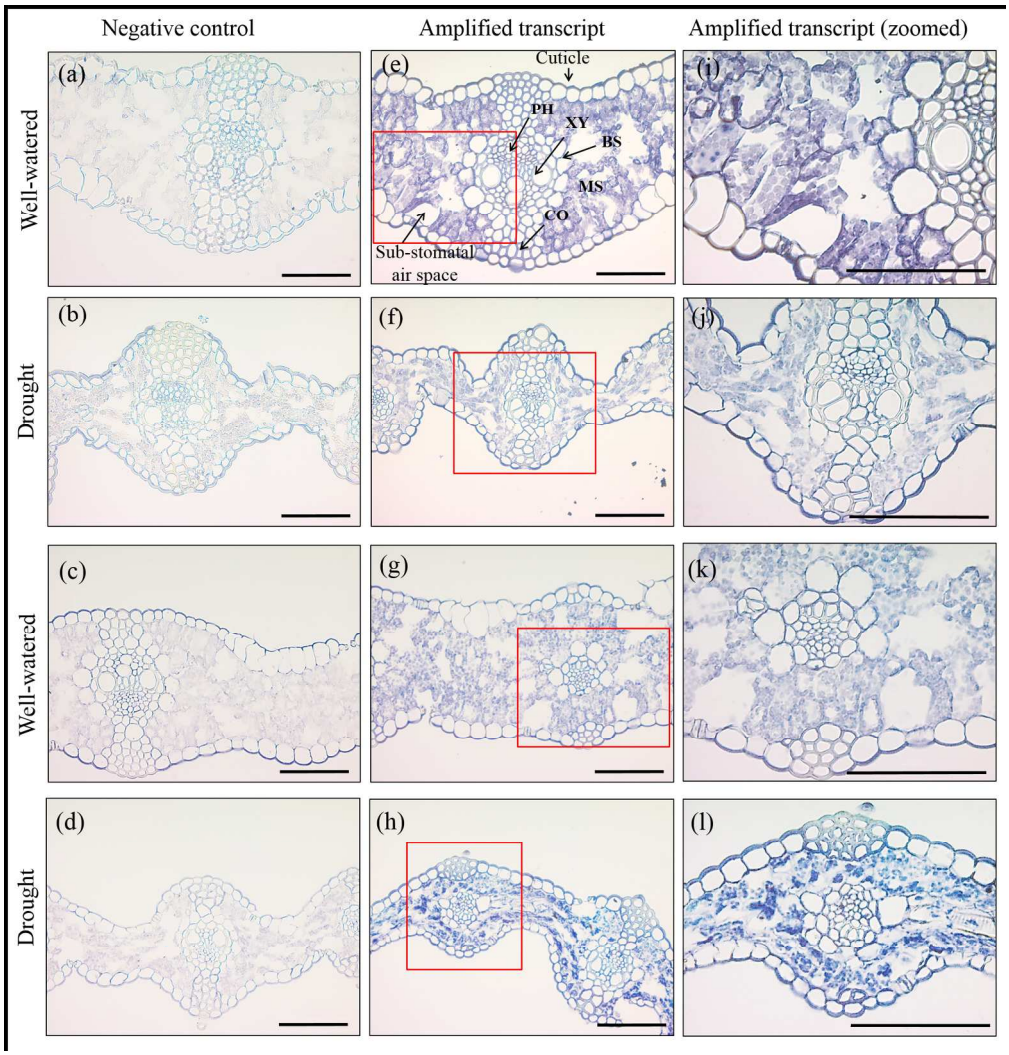

Figure 6. Light micrographs of the expression of *Osa*-miR1432 and the target transcript encoding Calmodulin-related (EF hand containing) calcium sensor protein by *in situ* PCR in Hindmarsh flag leaf sections from booting stage. Negative controls of miR1432 are shown in (a) well-watered and (b) drought treated samples. Negative controls of the target transcript are shown in (c) well-watered and (d) drought treated samples. miR1432 expression is shown in (e) well-watered and (f) drought treated samples. The target transcript expression is shown in (g) well-watered and (h) drought treated samples. Magnified view of the red boxed area of respective middle panel is shown the right panel (i-l). The blue stain indicates the presence of transcripts. Scale bar is 100µm. PH, phloem; XY, xylem; BS, bundle sheath; CO, collenchyma, MS, mesophyll cells.
339x354mm (150 x 150 DPI)